PERGAMON

International Journal of Solids and Structures 36 (1999) 311–337

INTERNATIONAL JOURNAL OF SOLIDS and STRUCTURES

A consistent equilibrium in a cross-section of an elastic–plastic beam

B. Vratanar, M. Saje

University of Ljubljana, Faculty of Civil and Geodetic Engineering, Jamova 2, SI-1115 Ljubljana, Slovenia

Received 26 June 1997; in revised form 10 October 1997

Abstract

A phenomenon of inequality of equilibrium and constitutive internal forces in a cross-section of elastic–plastic beams is common to many finite element formulations. It is here discussed in a rate-independent, elastic–plastic beam context, and a possible treatment is presented. The starting point of our discussion is Reissner's finite-strain beam theory, and its finite element implementation. The questions of the consistency of interpolations for displacements and rotations, and the related locking phenomena are fully avoided by considering the rotation function of the centroid axis of a beam as the only unknown function of the problem. Approximate equilibrium equations are derived by the use of the distribution theory in conjunction with the collocation method. The novelty of our formulation is an inclusion of a balance function that "measures" the error between the equilibrium and constitutive bending moments in a cross-section. An advantage of the present approach is that the locations, where the balance of equilibrium and constitutive moments should be satisfied, can be prescribed in advance. In order to minimize the error, explicit analytical expressions are used for the constitutive forces; for a rectangular cross-section and bilinear constitutive law, they are given in Appendix A. The comparison between the results of the two finite element formulations, the one using consistent, and the other inconsistent equilibrium in a cross-section, is shown for a cantilever beam subjected to a point load. The problem of high curvature gradients in a plastified region is also discussed and solved by using an adapted collocation method, in which the coordinate system is transformed such to follow high gradients of curvature.

1. Introduction

Inequality of stresses determined from equilibrium equations, and those obtained from constitutive equations is common to a majority of standard finite element formulations. This also holds true for cross-sectional stress-resultants of beams and shells. It appears that the phenomenon of the stress-inequality has not received much publicity so far. In the present paper, the phenomenon of the inequality of equilibrium-based and constitutive equations-based stress-resultants in finite element formulations, here termed the "inconsistent equilibrium", is discussed in detail in the context of a planar, finite-strain, elastic–plastic beam. The starting point of our discussion is

0020-7683/99/$—see front matter
PII: S0020-7683(97)00327-2

Reissner's (1972) finite-strain beam theory, and its finite element implementation given by Saje (1990) and Saje et al. (1997) which considers the rotation function of the centroid axis of a beam to be the only unknown function of the problem. In their formulations, only the inconsistency of bending moments occurs, while axial and shear forces are consistently equilibrated in an at least pointwise manner. A natural approach to fulfil the consistency condition of the bending moment in a pointwise manner is the collocation method, which is adopted as a basis of a numerical solution in the present paper. Consequently, the locations where the balance of equilibrium and constitutive moments should be satisfied can simply be prescribed in advance. In addition, we show that by employing an adapted collocation method in which the coordinate system is transformed in such a way that the solution follows high gradients of the curvature, yields more physically acceptable results in comparison to standard techniques.

In an analytical solution, the consistency of internal forces is automatically fulfilled. Yet an analytical solution of a beam accounting for exact geometric constraints, general boundary conditions, and the elastic–plastic constitutive law is not known. Only for a few geometrically and materially simple examples the researchers have managed to obtain a solution in a closed form. Reid and Reddy (1978) presented a limit analysis of a cantilever, where they assumed that the deformation was predominantly inextensional. Their results show a good agreement with an experiment presented therein. A similar problem was handled by Yu and Johnson (1982a), and Wu and Yu (1986). Again, these authors only considered the elastic–perfectly plastic constitutive law, and inextensional beam theory. An impressive solution of the cantilever problem is given by Liu et al. (1989); a strain-hardening model is considered in their analysis, but they still disregard the effect of the extensional strain. An analytical solution of the elastic–plastic cantilever beam accounting also for the effects of axial and transverse deformations, has not appeared yet. For the numerical treatment of the cantilever beam, the reader is directed to papers by Monasa (1980) and Fried (1985), among a variety of others.

In a numerical treatment applying standard finite element techniques, internal forces (or stresses) determined from equilibrium equations differ from those obtained from strains by using constitutive equations. This inequality between equilibrium and constitutive internal forces is usually tacitly ignored, and internal forces are often evaluated only from constitutive equations without a reference to equilibrium equations, or vice versa. For elastic material and small deformations, the discrepancies between constitutive and equilibrium quantities are usually small even for coarse finite element meshes, and can normally be disregarded. By contrast, for elastic–plastic material and large deformations, the differences cannot always be ignored, and do not vanish even for finer finite element meshes (Saje et al., 1996).

A key point of the present paper is the definition of the balance function of the cross-section of the beam, which "measures" the error between the equilibrium and the constitutive bending moment in a cross-section. By the use of the distribution theory in conjunction with the collocation approximation method the governing equilibrium equations are consistently approximated and the pointwise balance of the cross-sectional forces is assured in the set of collocation points. The present formulation employs the collocation method; its extension to account for other methods, e.g., Galerkin's method, the least squares method, is, however, straightforward, due to the generality of the distributional approximation operator. The formulation is also not restricted by the adopted material model.

In order to eliminate any error in computing constitutive forces and to minimize the overall

error, exact closed-form analytical expressions are derived for cross-sectional elastic–plastic parameters, i.e. the axial constitutive force, the extensional strain, the constitutive bending moment, and the constitutive matrix as functions of the axial force and the pseudocurvature.

The paper is organized as follows. In Section 2, we outline the governing equations of planar beams accounting for flexural, extensional, and shear effects. The corresponding natural and essential boundary conditions are also presented. A source of inconsistency of bending moments is discussed in Section 3. The derivation of the discrete approximate equilibrium equations is also presented in this section along with the balance conditions for the equilibrium and constitutive moments at the set of collocation points. Numerical results are shown in Section 4. Conclusions are given in Section 5. The paper ends with two appendices. Explicit expressions of elastic–plastic cross-sectional parameters are given in Appendix A, and nonvanishing elements of the Jacobian matrix of approximate equilibrium equations, needed for the solution by Newton's method, are presented in Appendix B.

2. Formulation of governing equations

We consider a straight, planar, elastic–plastic beam of initial length L and of cross-section A, subjected to the action of distributed loads $\mathscr{P}_x$, $\mathscr{P}_z$, and $\mathscr{M}$ along its span, and concentrated generalized forces S_k ($k = 1, \ldots, 6$) at the ends of the beam. Let the beam be analyzed in the (X, Z) plane of a fixed Cartesian coordinate system with unit base vectors $\mathbf{i}$, $\mathbf{k}$, and j, where $\mathbf{j} = \mathbf{k} \times \mathbf{i}$. The shape of the cross-section of the beam, and material distribution over the cross-section are assumed to be symmetric with respect to axis Z, but otherwise arbitrary. Extensional, bending, and shear strains are assumed to exist in the beam.

The configuration of a centroid axis of the beam is defined by a vector-valued function

$$\mathbf{r}: x \mapsto \mathbf{r}(x) = X(x)\mathbf{i} + Z(x)\mathbf{k} \quad (-1 \leqslant x \leqslant 1),$$

which generally represents the plane curve or, in the present case, the deformed line of the centroid axis of the beam, x is the nondimensional material coordinate of the centroid axis in the reference (undeformed or stress-free) space, and X, Z are spatial Cartesian coordinates of the axis.

Vector-valued function $\mathbf{r}$ is related to geometrical and deformation variables of the beam by the equations derived by Reissner (1972):

$$\mathbf{r}'(x) \equiv \begin{bmatrix} \frac{1}{2}L + u'(x) \\ w'(x) \end{bmatrix} = \frac{L}{2}\begin{bmatrix} (1+\varepsilon)\cos\varphi + \gamma\sin\varphi \\ -(1+\varepsilon)\sin\varphi + \gamma\cos\varphi \end{bmatrix}. \tag{1}$$

Here, the prime ($'$) denotes the derivative with respect to x. In (1) functions u and w denote displacements of the particle x in the spatial coordinate directions $\mathbf{i}$ and $\mathbf{k}$, respectively, whereas functions ε (notice that $\varepsilon(x) > -1$), γ, and φ denote the extensional strain (i.e. the specific axial elongation), the shear strain, and the rotation of the centroid axis, respectively. Equation (1) is termed the *geometrical* constraint.

Functions u, w, and φ will here be termed *geometrical* variables, since they determine the *geometrical configuration space* (u, w, φ) of a planar beam. Similarly, functions ε, γ, and φ', which are the generalized strains of our problem, span the *deformation configuration space* $(\varepsilon, \gamma, \varphi')$ within

the rigid displacement. Here, they will be termed deformation variables. Note the space duality of functions φ and φ' which are trivially related. Function φ' will also be termed the *pseudocurvature*, since in the special case $\varepsilon(x) = \gamma(x) = 0$ the curvature $\kappa(x) = \|\mathbf{r}'(x) \times \mathbf{r}''(x)\|/\|\mathbf{r}'(x)\|^3$ of the deformed line of the centroid axis,

$$\kappa(x) = \frac{2}{L} \frac{|(1+\varepsilon)^2\varphi' - (1+\varepsilon)\gamma' + \gamma\varepsilon' + \gamma^2\varphi'|}{((1+\varepsilon)^2 + \gamma^2)^{3/2}}, \tag{2}$$

reduces to $2|\varphi'(x)|/L$.

The governing equations of the beam can be obtained using, e.g., the generalized principle of virtual work. For the details of the derivation, the reader is directed to, e.g., Saje et al. (1997) or Antman and Rosenfeld (1978).

The geometrical constraints and the equilibrium equations are $(-1 < x < 1)$:

$$1 + \frac{2}{L}u' - (1+\varepsilon)\cos\varphi - \gamma\sin\varphi = 0, \tag{3a}$$

$$\frac{2}{L}w' + (1+\varepsilon)\sin\varphi - \gamma\cos\varphi = 0, \tag{3b}$$

$$\frac{2}{L}\Lambda_1' + \mathscr{P}_x = 0, \tag{3c}$$

$$\frac{2}{L}\Lambda_2' + \mathscr{P}_z = 0, \tag{3d}$$

$$\frac{2}{L}M' - (1+\varepsilon)Q + \gamma N + \mathscr{M} = 0, \tag{3e}$$

$$N - \Lambda_1\cos\varphi + \Lambda_2\sin\varphi = 0 \quad (-1 \leqslant x \leqslant 1), \tag{3f}$$

$$Q - \Lambda_1\sin\varphi - \Lambda_2\cos\varphi = 0 \quad (-1 \leqslant x \leqslant 1), \tag{3g}$$

where the pairs (Λ_1, Λ_2) and (N, Q) denote, respectively, vectors of equilibrium internal forces of a cross-section with respect to the fixed coordinate basis $\mathbf{i}$, $\mathbf{k}$, and with respect to the rotated coordinate system spanned by unit orthogonal vectors $(\cos\varphi, -\sin\varphi)$ and $(\sin\varphi, \cos\varphi)$. Function M is the equilibrium bending moment.

System (3) forms a set of seven equations for unknown functions u, w, φ, ε, γ, Λ_1, Λ_2, N, Q, and M. Notice that (3f) and (3g) are not differential equations and apply on the whole interval $[-1, 1]$.

The corresponding natural and essential boundary conditions are, $x \in \{-1, 1\}$:

$$\Lambda_1(-1) + S_1 = 0 \quad \text{or} \quad u(-1) = u_1, \tag{4a}$$

$$\Lambda_2(-1) + S_2 = 0 \quad \text{or} \quad w(-1) = u_2, \tag{4b}$$

$$M(-1) + S_3 = 0 \quad \text{or} \quad \varphi(-1) = u_3, \tag{4c}$$

$$\Lambda_1(1) - S_4 = 0 \quad \text{or} \quad u(1) = u_4, \tag{4d}$$

$$\Lambda_2(1) - S_5 = 0 \quad \text{or} \quad w(1) = u_5, \tag{4e}$$

$$M(1)-S_6=0 \quad \text{or} \quad \varphi(1)=u_6. \tag{4f}$$

To relate equilibrium forces N, Q, and equilibrium bending moment M to a material model, we introduce the final set of equations of the beam which assure the balance of equilibrium and constitutive cross-sectional forces and the bending moment, Antman and Rosenfeld (1978):

$$N(x,\Lambda_1(x),\Lambda_2(x),\varphi(x))=N_C(x,\varepsilon(x),\gamma(x),\varphi'(x)), \tag{5a}$$

$$Q(x,\Lambda_1(x),\Lambda_2(x),\varphi(x))=Q_C(x,\varepsilon(x),\gamma(x),\varphi'(x)), \tag{5b}$$

$$M(x,\Lambda_1(x),\Lambda_2(x),\varphi(x))=M_C(x,\varepsilon(x),\gamma(x),\varphi'(x)). \tag{5c}$$

Constitutive functions N_C, Q_C, and M_C define cross-sectional true stress-resultants—axial and transverse constitutive forces and the constitutive bending moment as functions of x. This form of constitutive eqns (5) must at least be invariant under rigid motions. Other constraints to (5), defined by Antman and Rosenfeld (1978), are automatically satisfied if constitutive functions (5) are derived from true stress–strain material model as herein. Notice that the constitutive forces in (5a) and (5b) are defined with respect to the same coordinate system as the equilibrium ones.

System of eqns (3) and (5) forms a total set of ten equations of the beam for unknowns of the problem and must be solved jointly with the boundary conditions (4).

Notice from (5) that constitutive functions must only depend on deformation variables ε, γ, and φ' and are subordinate to the adopted constitutive model, which is, in our case, defined by the uniaxial true stress–strain relation

$$\sigma(D)=\begin{cases} DE, & |D|\leqslant\varepsilon_Y \\ DE_p+\varepsilon_Y(E-E_p)\operatorname{sign} D, & |D|>\varepsilon_Y \end{cases} \tag{6}$$

and by a shear law which will be defined later. Here, E and E_p denote the elastic and plastic tangent modulus of material, ε_Y is the yield strain, and $D(x,z)=\varepsilon(x)+2z\varphi'(x)/L$ is the extensional strain of the cross-sectional point with nondimensional material coordinate $x\in(-1,1)$ and physical coordinates (y,z) of the cross-section, $(y,z)\in A$. For the sake of simplicity, unloading of material is not considered in the present discussion.

The constitutive functions are given by well known relations (see, e.g., Saje et al., 1997)

$$N_C(x,\varepsilon(x),\varphi'(x))=\int_A \sigma(x,z)\,\mathrm{d}A, \tag{7a}$$

$$Q_C(x,\gamma(x))=\int_A \tau(x,z)\,\mathrm{d}A=A_G\gamma(x), \tag{7b}$$

$$M_C(x,\varepsilon(x),\varphi'(x))=\int_A z\sigma(x,z)\,\mathrm{d}A. \tag{7c}$$

Here, σ is defined by (6), while τ is the true shear stress in the cross-section. The simplest constitutive model for the shear strain is adopted here, such that $Q_C=A_G\gamma$; A_G is the tangent shear stiffness of the cross-section, defined by $A_G=GA_s>0$, where G is shear modulus of material and $A_s<A$ the area of the shear cross-section (see Cowper, 1966). See Appendix A for explicit expressions of N_C,

M_C, and constitutive matrix $\mathbf{C}$ as functions of ε and φ' in case of a rectangular cross-section b/h, where full dependence on (6) is taken into account.

Let us analyze the consequences of eqns (5) and (7)! First, let us assume for the sake of simplicity of the argument, that Λ_1 and Λ_2 are functions of x only. It follows from (3c) and (3d) that this is so when distributed loads $\mathscr{P}_x$ and $\mathscr{P}_z$ are solely functions of x. Then (5a) and (5b), and the implicit function theorem imply that

$$\begin{aligned} \varepsilon &= \varepsilon(x, \Lambda_1(x), \Lambda_2(x), \varphi(x), \varphi'(x)), \\ \gamma &= \gamma(x, \Lambda_1(x), \Lambda_2(x), \varphi(x), \varphi'(x)). \end{aligned} \tag{8}$$

The problem can therefore be simplified such that only function φ is the unknown of the problem—see Saje (1990, 1991) in the context of elastic material, and Saje et al. (1997) for elastic–plastic material model. An analogous conclusion is derived, if $\mathscr{P}_x$ and $\mathscr{P}_z$ are only functions of φ or its derivative φ'.

By contrast, the explicit separation of the deformation variables by using (5) cannot be accomplished, if a general dependence of the distributed loads on, e.g., displacements is taken into account, i.e. if

$$\begin{aligned} \mathscr{P}_x &= \mathscr{P}_x(x, u(x), w(x), \varphi(x), \varepsilon(x), \gamma(x), \varphi'(x)), \\ \mathscr{P}_z &= \mathscr{P}_z(x, u(x), w(x), \varphi(x), \varepsilon(x), \gamma(x), \varphi'(x)). \end{aligned} \tag{9}$$

These relations generally mark the nonconservative load. In the case of nonconservative loads (9), it follows from (3c) and (3d) that Λ_1 and Λ_2 are functions of geometrical and deformation variables, and therefore the explicit separation of deformation variables ε, γ, and φ' (or φ because of its duality) using (5) is not feasible, since two nonlinear integro-differential equations, obtained from (5a) and (5b), must be simultaneously solved for ε and γ.

The question of an optimal choice of functions to be basic unknowns of the problem still remains open. A common practice is to take geometrical variables u, w, and φ as unknown functions of the problem. But Saje (1990, 1991) and Saje et al. (1997) showed that not only the number of unknowns is reduced but also the accuracy is improved, if only function φ is taken to be the unknown of the problem. This indicates that it would be more natural to choose the deformation variables than geometrical variables as the unknowns of the problem, especially in the case of the general dependence on distributed loads as in (9).

3. The consistent equilibrium in a cross-section

Prior to deriving discrete approximate equilibrium equations of the beam, let us discuss system (3) in more detail. In the analysis, we restrict ourselves to the case $\mathscr{P}_x = \mathscr{P}_x(x)$, $\mathscr{P}_z = \mathscr{P}_z(x)$, and $\mathscr{M} = \mathscr{M}(x)$, i.e. to conservative distributed loads. Please observe from (3) that some of the unknown functions can then be solved analytically.

In fact, the integration of (3c) and (3d) gives

$$\Lambda_1(x) = \Lambda_1(-1) - \frac{L}{2}\int_{-1}^{x} \mathscr{P}_x(\xi)\,\mathrm{d}\xi,$$
$$\Lambda_2(x) = \Lambda_2(-1) - \frac{L}{2}\int_{-1}^{x} \mathscr{P}_z(\xi)\,\mathrm{d}\xi, \qquad (-1 \leqslant x \leqslant 1). \tag{10}$$

In order to simplify the notation, it will be useful to set $\Lambda_1^0 = \Lambda_1(-1)$ and $\Lambda_2^0 = \Lambda_2(-1)$.

By the integration of geometrical constraints (3a) and (3b) we obtain

$$u(x) = u(-1) - L\frac{x+1}{2} + \frac{L}{2}\int_{-1}^{x} (1+\varepsilon)\cos\varphi\,\mathrm{d}\xi + \frac{L}{2}\int_{-1}^{x} \gamma\sin\varphi\,\mathrm{d}\xi,$$
$$w(x) = w(-1) - \frac{L}{2}\int_{-1}^{x} (1+\varepsilon)\sin\varphi\,\mathrm{d}\xi + \frac{L}{2}\int_{-1}^{x} \gamma\cos\varphi\,\mathrm{d}\xi, \tag{11}$$

where $x \in [-1, 1]$.

Equations (3f) and (3g) can analytically be solved, too, to obtain

$$N = N(x, \Lambda_1^0, \Lambda_2^0, \varphi(x)),$$
$$Q = Q(x, \Lambda_1^0, \Lambda_2^0, \varphi(x)). \tag{12}$$

Furthermore, (5a) is employed to derive ε (refer to Appendix A) as a function of x, N, and φ'. In the same way, function γ is obtained from (5b). To sum up, applying (10) in (5a), (5b), and (8), we obtain

$$\varepsilon = \varepsilon(x, N(x, \Lambda_1^0, \Lambda_2^0, \varphi(x)), \varphi'(x)),$$
$$\gamma = \gamma(x, Q(x, \Lambda_1^0, \Lambda_2^0, \varphi(x)). \tag{13}$$

Finally, the identity (5c) is employed to substitute equilibrium bending moment M in eqn (3e) with constitutive one M_C. As a result, only (3e) must numerically be solved for function φ.

Notice that (10)–(13) hold for any approximation of function φ.

A finite element formulation of governing equilibrium eqns (3)–(5) can be obtained by introducing an approximation of the unknown functions, which in our case takes the form

$$\varphi(x) \doteq \tilde{\varphi}(x, \mathbf{y}) = \sum_{k=1}^{n} P_k(x)\, y_k \quad (-1 \leqslant x \leqslant 1), \tag{14}$$

where P_k $(k = 1, \ldots, n)$ are the interpolation functions, and $\mathbf{y} = (y_1, \ldots, y_n)$ is the vector of independent parameters. Furthermore, we demand that the interpolation functions satisfy the essential boundary conditions

$$\tilde{\varphi}(-1, \mathbf{y}) = u_3, \quad \text{and} \quad \tilde{\varphi}(1, \mathbf{y}) = u_6. \tag{15}$$

In the sequel, we will equivalently use the notations $y_1 \equiv u_3$ and $y_n \equiv u_6$. Equations (15) require $P_1(-1) = P_n(1) = 1$, and $P_k(-1) = 0$ $(k = 2, \ldots, n)$, $P_k(1) = 0$ $(k = 1, \ldots, n-1)$.

In the papers by Saje (1990, 1991) and Saje et al. (1996, 1997), the Galerkin-type finite element method is applied to eqns (3), (5), and corresponding boundary conditions (4). As a consequence,

the numerical results in Saje et al. (1996, 1997) exhibit the inequality of the two bending moments $M(x)$ and $M_C(x)$ at cross-sections $x\in[-1,1]$. The source of this inequality stems from eqn (3e), which is there solved by using (5c) to obtain the equation

$$\phi'(x) = M'_C(x) - \frac{L}{2}((1+\varepsilon)Q - \gamma N - \mathscr{M}) = 0, \tag{16}$$

which in the course of the finite element procedure is required to vanish on the whole interval $(-1,1)$. Notice that (16) equalizes derivatives of M and M_C at point x, i.e. $\phi'(x) = M'_C(x) - M'(x) = 0$ for all $x\in(-1,1)$. Consequently and irrespective of the applied approximation method within a finite element, the primitive function $\phi(x)$ cannot be equal to zero, or equivalently, eqn (5c) cannot be realized by employing (16). Function ϕ is here termed the *balance* (or test) function of the bending moments.

By contrast, the consistent equilibrium of the bending moment in the cross-section is achieved by considering (5c) and integrating (3e)

$$\phi(x) = M_C(x) - M(a) - \frac{L}{2}\int_a^x ((1+\varepsilon)Q - \gamma N - \mathscr{M})\,\mathrm{d}\xi = 0 \quad (-1 \leqslant a, x \leqslant 1) \tag{17}$$

and solving numerically eqn (17) and not its derivative (16), i.e. $\phi(x) = M_C(x) - M(x) = 0$ for all $x\in[-1,1]$. Therefore, the cross-sectional equilibrium of all internal forces of the beam defined by (5) is definitely assured by (13) and (17). Notice that (13) applies for every $x\in[-1,1]$ on account of (14). If $\phi(x) = 0$ for all x in interval $[-1,1]$ then, in this case, $\tilde{\varphi}$ is equal to the analytical solution φ. However, if approximation (14) is introduced, (17) does not hold true for all x in the interval. Consequently, the balance function, ϕ, can be employed to measure the error (or distance) between the two bending moments in the cross-section by considering ϕ as an element of a Banach space. The balance function can also be applied to measure the local as well as the global error of the proposed finite element method. We say that a numerical method for solving (17) is *consistent*, if (17) is satisfied in a prescribed number of points of interval $[-1,1]$.

Combining (17) with equilibrium eqns (3) and boundary conditions (4) gives the set of approximate generalized equilibrium equations of the beam:

$$g_1(\Lambda_1^0, \Lambda_2^0, \mathbf{y}, u_1, u_4) = L + u_4 - u_1 - \frac{L}{2}\int_{-1}^{1}(1+\varepsilon)\cos\tilde{\varphi}\,\mathrm{d}x - \frac{L}{2}\int_{-1}^{1}\gamma\sin\tilde{\varphi}\,\mathrm{d}x = 0, \tag{18a}$$

$$g_2(\Lambda_1^0, \Lambda_2^0, \mathbf{y}, u_2, u_5) = u_5 - u_2 + \frac{L}{2}\int_{-1}^{1}(1+\varepsilon)\sin\tilde{\varphi}\,\mathrm{d}x - \frac{L}{2}\int_{-1}^{1}\gamma\cos\tilde{\varphi}\,\mathrm{d}x = 0, \tag{18b}$$

$$g_{k+2}(\Lambda_1^0, \Lambda_2^0, \mathbf{y}) = \langle T_k, \phi\rangle = 0 \quad (k = 1, \ldots, n), \tag{18c}$$

$$g_{n+3}(\Lambda_1^0) = \Lambda_1^0 + S_1 = 0, \tag{18d}$$

$$g_{n+4}(\Lambda_2^0) = \Lambda_2^0 + S_2 = 0, \tag{18e}$$

$$g_{n+5}(\Lambda_1^0) = \Lambda_1^0 - \frac{L}{2}\int_{-1}^{1}\mathscr{P}_x(x)\,\mathrm{d}x - S_4 = 0, \tag{18f}$$

$$g_{n+6}(\Lambda_2^0) = \Lambda_2^0 - \frac{L}{2}\int_{-1}^{1} \mathscr{P}_z(x)\,\mathrm{d}x - S_5 = 0. \tag{18g}$$

Equations (18) constitute the system of $n+6$ nonlinear equilibrium equations for unknowns Λ_1^0, Λ_2^0, u_1, u_2, $u_3 \equiv y_1$, u_4, u_5, $u_6 \equiv y_n$, and vector $\mathbf{y}$. The approximation method is here still arbitrary; therefore, the approximation operator to be applied on (17) is denoted by T_k $(k = 1, \ldots, n)$—refer to, e.g., Zemanian (1987). Standard approximation methods like spectral or pseudospectral methods can easily be considered through appropriate forms of operators T_k $(k = 1, \ldots, n)$. Natural boundary conditions (4c) and (4f) for boundary moments should also be incorporated in (18c).

Probably the most natural way to solve balance eqn (17) or (18c) is to apply the collocation method (sometimes also called the pseudospectral method). This will further be discussed later. Then the balance of bending moments (5c) is automatically achieved (in a pointwise manner) in a set of collocation points $\{x_k\}_{k\in I_{n+1}}$ in the interval $[-1, 1]$, where the index set is $I_{n+1} = \{0, \ldots, n\}$. Refer, e.g., to Lucas and Reddien Jr (1972), and Russell and Shampine (1972) for the mathematical background of the application of the collocation method in nonlinear problems, and, for instance, to Bayliss and Matkowsky (1987), Guillard and Peyret (1988), and Bayliss et al. (1989) for applications to physics problems.

Collocation points must, in our case, satisfy the following condition

$$-1 = x_0 \leqslant x_1 < \ldots < x_{n-1} \leqslant x_n = 1, \tag{19}$$

otherwise being arbitrary. If $x_0 = x_1$ and $x_{n-1} = x_n$, the natural boundary conditions (4c) and (4f) are automatically accounted for in (18). Otherwise, an additional error is introduced in system (18) (see Section 4).

In the collocation method, the approximation operator T_k is defined by

$$T_k = \delta_{x_k} - \delta_{x_{k-1}} \quad (k = 1, \ldots, n), \tag{20}$$

where δ denotes the δ-distribution (or the Dirac δ-function) with property $\langle \delta_a, \phi \rangle = \phi(a)$—refer to, e.g., Zemanian (1987). The reason for such a definition of T_k $(k = 1, \ldots, n)$ is the integral in (17). By using (20), we reduce the balance of bending moments of the beam of length L (or interval $[-1, 1]$) to the balance of (17) within smaller intervals $[x_{k-1}, x_k]$ $(k = 1, \ldots, n)$ between adjacent collocation points. This property of (20) is particularly important if the elastic–plastic constitutive model is taken into consideration, because the numerical integration along the axis in (17) or (18c) is prone to errors due to the presence of C^0-functions in the integrand (see Appendices A and B), refer also to Saje et al. (1997), Tvergaard and Needleman (1980), and Hutchinson and Koiter (1970). The same set of quadrature points as in (18c) is also applied in integrating (18a), (18b), (18f), and (18g). Furthermore, the balance of bending moment is achieved in all collocation points.

System (18) is solved by Newton's iterative method. If

$$\mathbf{x} = (y_2, \ldots, y_{n-1}, \Lambda_1^0, \Lambda_2^0, u_1, u_2, u_3 \equiv y_1, u_4, u_5, u_6 \equiv y_n)$$

denotes the vector of unknowns, eqns (18) can be rewritten as

$$\mathbf{g}(\mathbf{x}) = \mathbf{0}, \tag{21}$$

where vector $\mathbf{g}$ combines $n+6$ nonlinear equations of (18). Newton's solution method requires a series of solutions of linearized systems

$$D\mathbf{g}(\mathbf{x}_i)\Delta\mathbf{x}_{i+1} = -\mathbf{g}(\mathbf{x}_i), \quad \mathbf{x}_{i+1} = \mathbf{x}_i + \Delta\mathbf{x}_{i+1}, \quad \text{and} \quad (i = 0, 1, \ldots) \tag{22}$$

until the required accuracy is achieved. In (22) $D\mathbf{g}(\mathbf{x})$ is the Jacobian matrix of function $\mathbf{g}$ at point $\mathbf{x}$ (see Appendix B), and $\Delta\mathbf{x}_{i+1}$ is the Newton correction in iteration $i+1$.

Notice that the distribution theory allows to define the following derivatives

$$\frac{\partial}{\partial(\cdot)}\langle T_k, \phi\rangle = \left\langle T_k, \frac{\partial\phi}{\partial(\cdot)} \right\rangle \quad (k = 1, \ldots, n).$$

These appear precisely in the Jacobian matrix of (21). To obtain elements of the Jacobian matrix which belong to (18c), we only have to derive $\partial\phi/\partial(\cdot)$ for any definition of approximation operator T_k $(k = 1, \ldots, n)$. The dot $(\cdot)$ denotes an element of vector $\mathbf{x}$.

4. Numerical examples

The principal aim of the present paper is to discuss the effect of inconsistency of the equilibrium and constitutive internal forces, and to propose a method that assures their equality, at least pointwise. We study the consistent equilibrium in the cross-section of an elastic–plastic planar beam, using the finite-strain theory. The adopted material model is in numerical examples taken for simplicity to be elastic–plastic; the formulation itself is though not restricted to this particular material model. The essential novelty of the present approach is the collocation-based solution of momentum equation in its integrated form (17) rather than in its differentiated form (16) as in Saje et al. (1996, 1997), where the Galerkin-type of solution was applied. The effect of this new formulation on the accuracy is investigated in this section.

In order to show the validity of the explicit expressions of constitutive functions given in Appendix A, and to illustrate the means to derive analytical solutions where also extensional strain ε is taken into account in the material model, we first consider a cantilever subjected to the point moment at its end. For this simple example, the analytical solution is derived. The effect of the inconsistent bending moment is assessed via the Coulter and Miller (1989) cantilever. The last example illustrates the problem of high gradients of the rotation function in the plastic region, its consequences to the accuracy of the solution, and a possible solution cure using an adaptive collocation procedure. In all examples, only one finite element is employed to model the whole cantilever.

4.1. *The cantilever subjected to the moment at the free end*

We consider a simple, but indicative example of the cantilever subjected to the concentrated free-end moment S_3—refer to, e.g. Reid and Reddy (1978), Yu and Johnson (1982a), Fried (1985), Wu and Yu (1986), and Liu et al. (1989). We assume homogeneous material throughout the whole cantilever.

The boundary conditions of this problem are:

$$\Lambda_1(-1) = 0, \qquad u(1) = 0, \tag{23a}$$

$$\Lambda_2(-1) = 0, \quad \text{and} \quad w(1) = 0, \tag{23b}$$

$$M(-1) + S_3 = 0, \qquad \varphi(1) = 0. \tag{23c}$$

Because $\mathscr{P}_x(x) = \mathscr{P}_z(x) = 0$ and $\Lambda_1(-1) = \Lambda_2(-1) = 0$, functions $\Lambda_1(x)$ and $\Lambda_2(x)$ vanish everywhere on the interval $[-1, 1]$. Consequently, the axial and transverse forces, N and Q, also vanish due to (3f) and (3g). It, therefore, follows from (13) or (A5)–(A7) that $\varepsilon(x) = \gamma(x) = 0$. Finally, eqn (3e) with $\mathscr{M}(x) = 0$ combined with the natural boundary condition (23c) gives the well known result for equilibrium moment $M(x) = -S_3$ $(-1 \leqslant x \leqslant 1)$.

To obtain geometrical variables u, w, and φ, the identity (5c) must be solved for $\varphi(x)$. Inserting $\varepsilon(x) = 0$ into (A8)–(A10) gives

$$0 = \begin{cases} \alpha_0 + \alpha_1 \varphi'(x), & |S_3| \leqslant M_Y \\ \beta_0 - \beta_1 \varphi'^2(x) + \beta_2 \varphi'^3(x), & |S_3| > M_Y \end{cases} \tag{24}$$

where $M_Y = \varepsilon_Y b h^2 E/6$ is the limit elastic moment, whereas coefficients in (24), along with the relation sign $\varphi' = -\text{sign}\, S_3$, are consecutively denoted by

$$\alpha_0 = S_3, \qquad \beta_0 = \varepsilon_Y^3 \frac{E - E_p}{3} b \,\text{sign}\, S_3,$$

$$\alpha_1 = E\frac{bh^3}{6L}, \quad \beta_1 = \varepsilon_Y \frac{E - E_p}{L^2} bh^2 \,\text{sign}\, S_3 - \frac{4S_3}{L^2},$$

$$\beta_2 = E_p \frac{2bh^3}{3L^3}.$$

If we define

$$M_p(x) = \varepsilon_Y \frac{E - E_p}{4} bh^2 + |\varphi'(x)| \frac{bh^3}{6L} E_p \tag{25}$$

as the ultimate constitutive bending moment, where $M_Y < M_p$, then the applied end moment is bounded such that $|S_3| < M_p$, since M_p is also the asymptotic function of M_c for $\varphi'(x) \to \infty$ and $\varepsilon(x) = 0$ [refer to (A10)].

It can easily be proven using the argument principle from complex analysis that (24) has only one real solution for function φ', on the half plane $\text{sign}\, S_3 \,\text{Re}\, z \leqslant 0$ $(S_3 \neq 0)$. Function φ is, therefore, given by

$$\varphi(x) = K(x-1) \quad (-1 \leqslant x \leqslant 1), \tag{26}$$

where constant K is the solution of (24). Inserting $\varphi'(x) = K$ into (2) yields $R = L/2K$, where $|R|$ is the radius of curvature of the deformed cantilever. Equation (26) shows that pseudocurvature $\varphi'(x)$ is constant for any load-level. Notice that (26) holds true also in the case of elastic springback of the beam, considered in Yu and Johnson (1982b).

The displacements of the centroid axis of the beam, $u(x)$ and $w(x)$, are obtained by the introduction of the essential boundary conditions (23a) and (23b) into (11):

$$u(x) = L\frac{1-x}{2} + \frac{L}{2K}\sin K(x-1)$$

$$w(x) = L\frac{\cos K(x-1)-1}{2K} \qquad (-1 \leqslant x \leqslant 1).$$

Finally, setting $X = L(1+x)/2+u(x)$ and $Z = w(x)$ yields

$$(X-L)^2+(Z+R)^2 = R^2. \tag{27}$$

Therefore, the deformed shape of the cantilever is in both cases, i.e. for elastic (see Saje and Srpčič, 1985) and elastic–plastic material, represented by a circle of radius $|R|$ with a centre at $(L, -R)$. Observe that (27) is also valid for the small-deformation theory. Our numerical solution using $n \geqslant 1$ collocation points, and irrespective of the integration scheme, is completely coincident with the analytical solution (27).

4.2. *The Coulter and Miller* (1989) *cantilever*

This example is presented and well documented by Coulter and Miller (1989) refer also to Saje et al. (1997). A cantilever of length $L = 50.8$ cm and of a square cross-section, $b = h = 1.27$ cm, is subjected to a transverse end-point load $S_2 = 1.78$ kN.

The following boundary conditions can be obtained from (4):

$$\Lambda_1(-1) = 0, \qquad u(1) = 0, \tag{28a}$$

$$\Lambda_2(-1)+S_2 = 0, \quad \text{and} \quad w(1) = 0, \tag{28b}$$

$$M(-1) = 0, \qquad \varphi(1) = 0. \tag{28c}$$

A material obeying a true stress–strain diagram given in (6) is employed having elastic modulus $E = 20692.5$ kN/cm^2, strain hardening modulus $E_p = 5173.1$ kN/cm^2, and extensional yield strain $\varepsilon_Y = 0.00147$; we assume shear-stiff cross-section $A_G \gg 0$, since Coulter and Miller (1989) neglect the influence of transverse force Q on deformation.

Interpolation functions P_k $(k = 1, \ldots, n)$ are taken to be the Lagrangian interpolation polynomials with equidistant interpolation points $\{x_k \mid x_k = -1+2k/r, k = 0, \ldots, r\}$

$$L_k^{(r)}(x) = \frac{(-1)^{r-k}\, r^r}{2^r r!}\binom{r}{k}\frac{\Pi(x)}{x-x_k} \qquad (k = 0, \ldots, r),$$

where r is the degree of polynomials and $\Pi(x) = (x-x_0)(x-x_1)\ldots(x-x_r)$. The Gaussian quadrature formulae for numerical integration along the axis are employed. Since the analytical solution for this problem has not yet been derived, results are compared with Saje et al. (1997). The error tolerance of Euclidean norm of vector $\mathbf{x}$ is in all cases taken to be 10^{-10}. As discussed in Section 3, the set of collocation points $\{x_k\}_{k\in I_{n+1}}$ can generally be prescribed at will. Thus we can control the location of collocation points such that the equilibrium and constitutive moments are equal in an optimum sense.

First we analyze the influence of the degree of numerical integration used. For this sake, we take $n = 8$ and consider $L_k^{(n)}$ $(k = 0, \ldots, n-1)$. The set of collocation points $\{x_1, \ldots, x_n\}$ is taken to be

Table 1
The influence of order n_G of the Gaussian integration along the axis on tip displacements $u(-1)$ and $w(-1)$, tip rotation $\tilde{\varphi}(-1)$, and curvature $\kappa(1)$. $\|\phi\|_2$ is L^2-norm of the balance function

n_G	$u(-1)$	$w(-1)$	$\tilde{\varphi}(-1)$	$\kappa(1)$	$\|\phi\|_2$
1	12.8266	31.1255	0.9241	0.0499	0.6565
2	12.8150	30.9968	0.9252	0.0499	0.4580
3	12.8153	30.9966	0.9252	0.0499	0.4865
4	12.8153	30.9966	0.9252	0.0499	0.4889

the Lobatto quadrature points, thus all requirements regarding boundary conditions are automatically satisfied (see Section 3). Table 1 presents the numerical values of tip displacements $u(-1)$ and $w(-1)$, rotation $\tilde{\varphi}(-1)$, curvature $\kappa(1)$, and L^2-norm of balance function ϕ as a function of the order of Gaussian quadrature formulae. Results in Table 1 show that no locking emerges in the present procedure and that the results using $n_G = 3$ and 4 coincide. For this particular example, researchers usually recommend the Lobatto quadrature formulae to capture correctly the plastic hinge that emerges at the end-point, $x = 1$. In the present approach, the type and the degree of numerical integration is not very essential, because the plastic hinge is fully incorporated into balance function (17) through the natural boundary conditions (4c) and (4f), and the choice of the collocation points (19).

The influence of the location of collocation points $\{x_1, \ldots, x_n\}$ is analyzed next. We take the same interpolation functions as before ($n = 8$), while the order of Gaussian quadrature formula is $n_G = 4$. Results for tip displacements $u(-1)$ and $w(-1)$, tip rotation $\tilde{\varphi}(-1)$, end-point curvature $\kappa(1)$, bending moments $M_C(-1)$, $M_C(1)$, and $M(1)$, and L^2-norm of balance function ϕ as a function of the location of collocation points are displayed in Table 2 for equidistant (E), $\{-1+2k/(n-1) \mid k = 0, \ldots, n-1\}$, Lobatto (L), Gaussian (G), and Chebyshev (C), $\{\cos(\pi k/(n-1)) \mid k = n-1, \ldots, 0\}$, collocation points. Good agreement is observed between various collocation schemes for displacements, rotation, and curvature. The balance of bending moments at $x = 1$ is achieved in the case of equidistant (E), Lobatto (L), and Chebyshev (C)

Table 2
The influence of the location of collocation points $\{x_k\}_{k \in I_{n+1}}$ on tip displacements $u(-1)$, $w(-1)$, tip rotation $\tilde{\varphi}(-1)$, end-point curvature $\kappa(1)$, and bending moments $M_C(-1)$, $M_C(1)$, and $M(1)$. $\|\phi\|_2$ is L^2-norm of the balance function

Type	$u(-1)$	$w(-1)$	$\tilde{\varphi}(-1)$	$\kappa(1)$	$M_C(-1)$	$M_C(1)$	$M(1)$	$\|\phi\|_2$
E	12.8016	30.9793	0.9278	0.0499	0.0000	−67.6372	−67.6372	1.5669
L	12.8153	30.9966	0.9252	0.0499	0.0000	−67.6128	−67.6128	0.4889
G	12.8123	30.9951	0.9248	0.0500	2.0340	−67.6928	−67.6181	0.5852
C	12.8168	30.9973	0.9256	0.0499	0.0000	−67.6101	−67.6101	0.4471

E—equidistant, L—Lobatto, G—Gaussian, C—Chebyshev.

collocation points, but not for Gaussian (G) collocation points. Please observe also from Table 2 that L^2-norm of the balance function varies for different choice of the location of the collocation points. Still, no sharp condition has been derived yet for the optimal position of collocation points. where some norm $\|\phi\|$ takes its minimum.

The effect of the order of interpolation functions $L_k^{(n)}$ $(k = 0, \ldots, n-1)$ is displayed in Table 3. The Gaussian integration of order $n_G = 4$ is used and Gaussian collocation points are employed. Results for tip displacements $u(-1)$ and $w(-1)$, tip rotation $\tilde{\varphi}(-1)$, end-point curvature $\kappa(1)$, bending moments $M_C(-1)$, $M_C(1)$, and $M(1)$, and L^2-norm of balance function ϕ as a function of n are given in Table 3. Observe that the Gauss collocation points do not meet requirements of the natural boundary condition (28c). It can also be observed from Table 3 that neither the error in balance of moments at $x = -1$ nor norm $\|\phi\|_2$ decrease uniformly by increasing the order of interpolation functions. Results from Saje et al. (1997) are, for the comparison sake, presented in Table 3.

The inequality of bending moments is inherent in the Galerkin-type of the finite element method and is well observed in Table 4 for $x = 1$, in particular for larger loads and using nonhardening material model ($E_p = 0$). Note that the exact ultimate constitutive bending moment is $M_p = 15.5769$ kNm. The error grows with load factor λ and is larger than 100% for $\lambda = 10$. This again shows the importance of the consistency of the equilibrium at large strains (cf Subsection 4.3).

4.3. *The Coulter and Miller* (1989) *cantilever—the problem of high gradients*

In an elastic–plastic beam, the rotation function may exhibit large gradients in highly localized plastified zones. For the cantilever subjected at its free end with a transverse point load (see Coulter and Miller, 1989), this takes place at its clamped end. When employing a standard polynomial interpolation for the rotation and irrespective of the numerical methods, the solution variables (the rotation, displacements, deformations, internal forces) may exhibit high oscillations along the axis of the beam which are of no physical ground. Although the amplitudes of oscillations may be

Table 3
Tip displacements $u(-1)$, $w(-1)$, tip rotation $\tilde{\varphi}(-1)$, end-point curvature $\kappa(1)$, and bending moments $M_C(-1)$, $M_C(1)$, and $M(1)$ as a function of n; $n_G = 4$; collocation points are Gaussian quadrature points. $\|\phi\|_2$ is L^2-norm of the balance function

n	$u(-1)$	$w(-1)$	$\tilde{\varphi}(-1)$	$\kappa(1)$	$M_C(-1)$	$M_C(1)$	$M(1)$	$\|\phi\|_2$
2	12.9097	30.8022	0.9088	0.0445	21.1256	−61.5229	−67.4448	11.2829
4	12.7927	30.9872	0.9239	0.0496	−5.4576	−67.2505	−67.6529	1.3462
6	12.8174	30.9975	0.9261	0.0501	−0.6410	−67.8823	−67.6091	0.5757
8	12.8123	30.9951	0.9248	0.0500	2.0340	−67.6928	−67.6181	0.5852
10	12.8121	30.9949	0.9250	0.0498	−1.0653	−67.5059	−67.6185	0.1919
12	12.8124	30.9951	0.9250	0.0499	−0.0918	−67.6530	−67.6179	0.1038
†	12.8153	30.9966	0.9252	0.0499	−0.0040	−67.6145	−67.6128	—

† Saje *et al.* (1997)—one element E_{8-8} (Lobatto integration).

Table 4.
The inequality of bending moments $M_C(1)$ vs $M(1)$ as a function of load factor λ using nonhardening material model $E_p = 0$ and equidistant collocation points; $n_G = 4$

λ	$M_C(1)$	$M_C(1)$†	$M(1)$[a]
0.1	−9.0361	−9.0361	−9.0361
0.2	−15.5764	−15.5768	−15.7420
0.3	−15.5768	−15.5769	−16.2937
0.5	−15.5768	−15.5769	−16.7257
1	−15.5768	−15.5769	−17.6947
3	−15.5769	−15.5769	−21.4605
5	−15.5769	−15.5769	−25.0931
10	−15.5769	−15.5769	−33.6533

[a] Saje *et al.* (1997)—one element E_{5_8} (Lobatto integration).

made somewhat smaller by using finer finite element meshes, the oscillations are never cancelled out using more finite elements.

A promising solution method for the high-gradient problems was suggested by Bayliss and Matkowsky (1987), and Guillard and Peyret (1988), and refined later on by Bayliss et al. (1989) in the context of the numerical integration of stiff partial differential equations, arising in problems such as the flame propagation and gasless combustion of a solid material. They introduced an adaptive Chebyshev collocation method such that by minimizing a Sobolev norm of an appropriate function, the spatial discretization error is substantially reduced. By prescribing an error bound of the solution vector, their procedures also allow to calculate the number of collocation points to maintain the prescribed error throughout a time domain.

The adaptive collocation method of Bayliss and Matkowsky (1987) is applied here for the solution of the high-gradient problem in an elastic–plastic beam. To show the oscillatory character of the standard collocation solution, we first present (i) the solution of the Coulter and Miller (1989) cantilever made of nonhardening material ($E_p = 0$) using standard Chebyshev polynomials $T_k(x)$ $(k = 0, \ldots, n)$, and then—to show a great improvement—(ii) the solution employing modified Chebyshev polynomials $T_k(\psi^{-1}(x))$ $(k = 0, \ldots, n)$ as described later on. In both cases $n = 9$, and the set of collocation points $\{x_1, \ldots, x_n\}$ is assumed to coincide with the Chebyshev and Gaussian quadrature points. Observe that the Chebyshev collocation points enable satisfying the natural boundary condition (28c), while the Gaussian collocation points do not. In both examples, the Gaussian integration with $n_G = 5$ is employed for the numerical integration along the axis.

The results using Chebyshev collocation points are shown in Figs 1 and 2. The standard Chebyshev interpolation polynomials are not capable of following the high gradients of φ at clamped point $x = 1$ for large loading factors λ, and exhibit oscillatory solution even for small loading factors, see Fig. 1 (dashed lines). Consequently, the deformed shapes of the cantilever, as depicted in Fig. 2 by dashed lines for various values of loading factor $\lambda = 0.18$, 0.2, 0.3, 0.5, 1.5, and 10, are also oscillatory and are, particularly for larger λ, evidently physically inadequate.

To improve the solution, we adopt the procedure similar to the one of Bayliss and Matkowsky

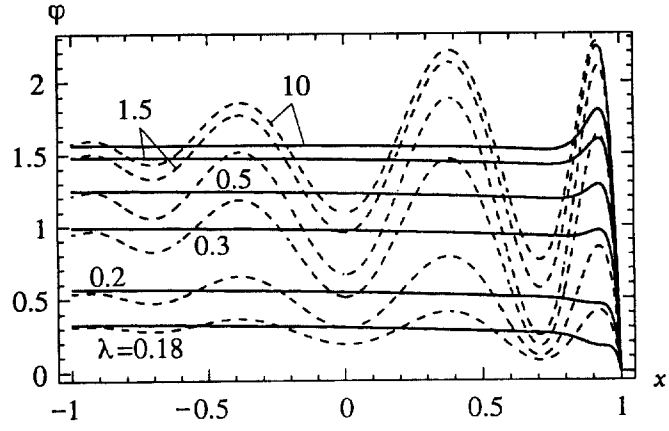

Fig. 1. Rotation $\varphi(x)$ $(-1 \leqslant x \leqslant 1)$ as a function of load factor λ. Interpolation function: dashed line—standard Chebyshev polynomials $T_k(x)$ $(k = 1, \ldots, 9)$; solid line—modified Chebyshev polynomials $T_k(\psi^{-1}(x))$ $(k = 1, \ldots, 9)$. Chebyshev collocation points.

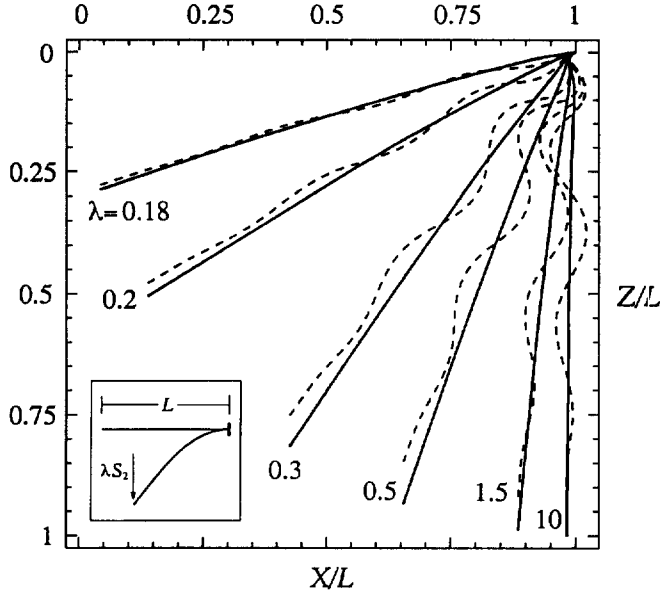

Fig. 2. Deformed shapes of the cantilever at various load factors λ. Interpolation function: dashed line—standard Chebyshev polynomial $T_k(x)$ $(k = 1, \ldots, 9)$; solid line—modified Chebyshev polynomials $T_k(\psi^{-1}(x))$ $(k = 1, \ldots, 9)$. Chebyshev collocation points.

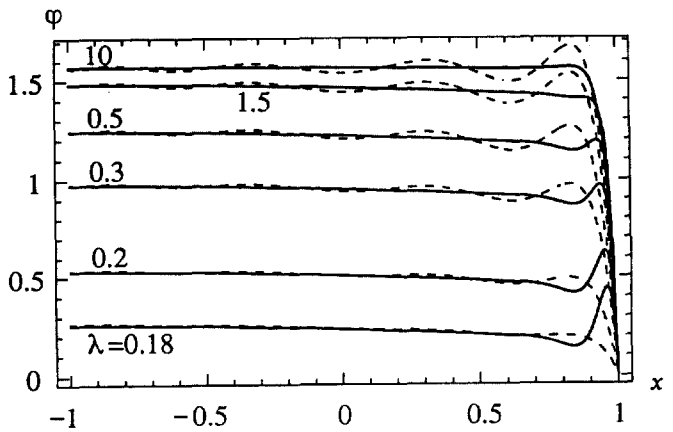

Fig. 3. Rotation $\varphi(x)$ $(-1 \leqslant x \leqslant 1)$ as a function of load factor λ. Interpolation function: dashed line—standard Chebyshev polynomials $T_k(x)$ $(k = 1, \ldots, 9)$; solid line—modified Chebyshev polynomials $T_k(\psi^{-1}(x))$ $(k = 1, \ldots, 9)$. Gaussian collocation points.

(1987) and introduce the change of the material coordinate system by the transformation ψ: $\hat{\Omega} \to \Omega$ defined by

$$\psi: s \mapsto x \equiv \psi(s) = \frac{4}{\pi} \arctan\left(\omega \tan \pi \frac{s-1}{4}\right) + 1 \quad (-1 \leqslant s, x \leqslant 1), \tag{29}$$

where $\omega > 0$ is the prescribed parameter, here taken to be constant for all loading factors, i.e. $\omega = 0.25$. The map (29) transforms a stiff problem in space $\Omega = [-1, 1]$, in our case system (18), to the less stiff problem in space $\hat{\Omega} = [-1, 1]$ where the standard Chebyshev polynomials $T_k(s)$ $(k = 0, \ldots, n)$ and adopted collocation points can be employed. Transformation (29) is not taken over the set of collocation points to avoid problems of interpolation of cross-sectional parameters if materials with memory are considered. The improvement of the results for rotation function φ and deformed shapes due to application of (29) is tremendous (refer to Figs 1 and 2; full lines) even for a one-finite element model. We note that the transformation function given in (29) is only one of the variety of possible choices. An optimal transformation function, which must embrace the location of the high gradients (usually the location of the highly plastified region), for the present problem is, however, not known.

The location of the collocation points is, however, very important in the solution to the problem of high gradients. This is well observed from Figs 3 and 4, where the Gaussian collocation points are considered, and from the comparison with Figs 1 and 2. The comparison shows that the Gaussian collocation points result in less oscillatory solution for higher loading factors. Notice from Fig. 3 that for smaller loading factors the presumption $\omega = 0.25$ for all loading factors is not accurate enough (the oscillations emerge). Generally, the parameter of the transformation (29), ω, should depend on the value of the load factor, $\omega = \omega(\lambda)$. This promising results indicate that further research would be reasonable.

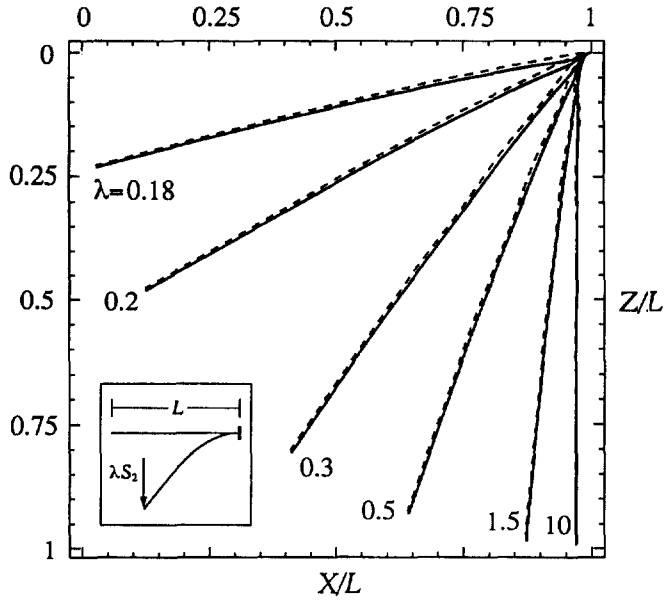

Fig. 4. Deformed shapes of the cantilever at various load factors λ. Interpolation function: dashed line—standard Chebyshev polynomial $T_k(x)$ $(k = 1,\ldots,9)$; solid line—modified Chebyshev polynomials $T_k(\psi^{-1}(x))$ $(k = 1,\ldots,9)$. Gaussian collocation points.

5. Conclusions

The phenomenon of the inequality of equilibrium-based and constitutive equations-based internal forces in finite element formulations, here termed the "inconsistent equilibrium", has been discussed in the context of a planar, finite-strain, rate-independent, elastic–plastic beam theory, and a possible solution to overcome this problem has been proposed which uses the collocation method.

First, the so-called "balance function" that "measures" the error between equilibrium and constitutive bending moments is introduced. It enables the control of the equilibrium in a cross-section as well as the local or global error of the proposed finite element method. Next, in contrast to standard finite element formulations, where approximate equilibrium equations are obtained by the variational principles, here we apply the distribution theory instead. This enables a broad range of approximation methods to be considered, e.g., Galerkin's, the least squares, and the collocation method. Here we adopt the collocation method as a basis of our numerical solution, because it represents a natural approach to fulfil the consistency condition in a pointwise manner. This method requires numerical integrations of the balance function between the collocation points. This is a computationally demanding operation, yet it enables considering very accurately constitutive laws where C^0-functions emerge; one of them is the elastic–plastic constitutive law. A further advantage of the collocation method is that the positions of collocation points within a finite element can be chosen such to capture regions of the highest strain gradients optimally.

Three examples are elaborated. In the first one, the analytical solution of an elastic–plastic

cantilever subjected to the end-point moment is given. The solution is a circle, as in the case of an elastic constitutive law.

The effect of unbalanced bending moments in a cross-section is systematically examined in the second example. We confirm, even in the elastic–plastic context, the absence of the locking phenomenon in the present numerical procedure, and show that no quadrature formula for numerical integration along the axis is privileged. By contrast, the locations of the collocation points are essential, especially in the highly localized plastified zones. They are chosen such that they enforce the balance of equilibrium and constitutive moments at desired locations. We used equidistant, Lobatto's, Gaussian, and Chebyshev's collocation points. An optimal positioning of collocation points, an optimal number of collocation points, a remeshing, and adaptivity algorithms have, however, not been considered in the present paper.

The third example concentrates on the problem of high gradients of the rotation function in a highly localized plastic zone, which typically occurs with an elastic–plastic constitutive law. The adaptive collocation method of Bayliss and Matkowsky (1987) is applied here and modified for the purpose of the present problems. The results of this adaptive procedure are noticeably physically more acceptable and promising. However, more research is needed to improve the solution further.

Acknowledgements

The authors are thankful to our colleague I. Planinc for his criticisms, comments, and helpful discussions. The work of B.V. has been financially supported by the Ministry of Science and Technology of the Republic of Slovenia under contract S12-0792-017/15161. The support is gratefully acknowledged.

Appendix A: Elastic–plastic parameters of the cross-section

Elastic–plastic parameters of a rectangular cross-section (b/h) are: N_C—the constitutive axial force, ε—the extensional strain of the axis, M_C—the constitutive bending moment, and $\mathbf{C}$—the cross-sectional constitutive matrix. For an idealized case, where the effects of axial and shear forces on the deformation are negligible, these parameters are given by, e.g., Reid and Reddy (1978), Monasa (1990), Yu and Johnson (1982a, 1982b), Fried (1985), Wu and Yu (1986) and Liu et al. (1989). We present here exact, closed-form explicit expressions for elastic–plastic parameters which also account for extensional strain ε and $E_p \geqslant 0$. They are based on constitutive law (6). To the authors' knowledge such expressions have not been published before.

To simplify the derivation and the notation, we assume the following nondimensional quantities

$$\alpha = \frac{E_p}{E}, \quad p = \frac{\varepsilon}{\varepsilon_Y}, \qquad n = \frac{N_C}{N_Y}, \quad \text{where } N_Y = \varepsilon_Y bhE,$$

$$k = \frac{h}{\varepsilon_Y L}\varphi', \quad m = \frac{M_C}{M_Y}, \quad \text{where } M_Y = \frac{1}{6}\varepsilon_Y bh^2 E.$$

Note that the forthcoming expressions for the constitutive forces hold true irrespective of the approximation (14).

A.1. The constitutive axial force, $N_C(x, \varepsilon(x), \varphi'(x)) = N_Y n(p, k, \alpha)$

The constitutive axial force, N_C, is introduced by (7a), where true stress $\sigma(D)$ is defined by (6). In deriving the analytical expression for n, we have to distinguish three cases: (i) $k = 0$. (ii) $|k| \leqslant 1$ with $k \neq 0$, and (iii) $|k| > 1$.

To distinguish, within each case, different states (elastic, elastic–plastic, and plastic) of the cross-section, we introduce the boundary values of nondimensional extensional strain p:

$$p_0 = 1, \quad p_1 = 1-|k|, \quad p_2 = 1+|k|, \quad p_3 = |k|-1. \tag{A1}$$

Therefore, for ($k = 0$ and $|p| \leqslant p_0$) or ($|k| \leqslant 1$ with $k \neq 0$ and $|p| \leqslant p_1$), the cross-section is in elastic state, whereas for ($k = 0$ and $|p| > p_0$) or ($k \neq 0$ and $|p| > p_2$), the whole cross-section is plastified. For all other combinations of k and p, the cross-section is partially elastic and partially plastic.

The separation points, $z_1(x)$ and $z_2(x)$, between elastic and plastic states are defined by conditions $D(x, z_1(x)) = \varepsilon_Y$ and $D(x, z_2(x)) = -\varepsilon_Y$, which give

$$z_1(x) = h\frac{1-p(x)}{2k(x)} \quad \text{and} \quad z_2(x) = -h\frac{1+p(x)}{2k(x)}.$$

It is clear that inequalities $|z_1(x)| < h/2$ and $|z_2(x)| < h/2$ must hold.

After inserting $z_1(x)$ and $z_2(x)$ into (7a) and introducing notations

$$a_0 = \frac{1-\alpha}{4|k|}, \quad a_1 = \frac{1+\alpha}{2} + \frac{1-\alpha}{2|k|}, \quad a_2 = \frac{1-\alpha}{4}\left(\frac{1}{|k|} + |k| - 2\right),$$

we obtain for $k = 0$:

$$n = \begin{cases} p, & |p| \leqslant p_0 \\ \alpha p + (1-\alpha)\operatorname{sign} p, & |p| > p_0 \end{cases} \tag{A2}$$

whereas for $|k| \leqslant 1$ and $k \neq 0$

$$n = \begin{cases} p, & |p| \leqslant p_1 \\ -a_0 p|p| + a_1 p - a_2 \operatorname{sign} p, & p_1 < |p| \leqslant p_2 \\ \alpha p + (1-\alpha)\operatorname{sign} p, & |p| > p_2. \end{cases} \tag{A3}$$

For $|k| > 1$, it yields

$$n = \begin{cases} p\left(\alpha + \dfrac{1-\alpha}{|k|}\right), & |p| \leqslant p_3 \\ -a_0 p|p| + a_1 p - a_2 \operatorname{sign} p, & p_3 < |p| \leqslant p_2 \\ \alpha p + (1-\alpha)\operatorname{sign} p, & |p| > p_2. \end{cases} \tag{A4}$$

Observe that (A2)–(A4) define a strictly monotonic function for $\alpha \neq 0$, so the inverse function of n with respect to p exists [cf (8)].

A.2. The extensional strain, $\varepsilon(x, N(x), \varphi'(x)) = \varepsilon_Y p(n, k, \alpha)$

Extensional strain ε as a function of n, k, and α can be derived by inversion of (A2)–(A4). The inversion of (A2)–(A4) is, however, possible only for $\alpha \neq 0$ (or $E_p \neq 0$), as already stated in Subsection A.1.

To obtain the inverse function, p, a domain, i.e., the state of the cross-section, must properly be modified. For this purpose, boundary values (A1), which define the domain of function n, must be replaced with their counterparts, the characteristic values of axial forces obtained from (A2)–(A4):

$$n_0 = 1, \quad n_1 = 1-|k|, \quad n_2 = 1+\alpha|k|, \quad n_3 = (|k|-1)\left(\alpha+\frac{1-\alpha}{|k|}\right).$$

Application of characteristic axial forces n_i $(i = 0, \ldots, 3)$ in (A2)–(A4) at $k = 0$ gives

$$p = \begin{cases} n, & |n| \leqslant n_0 \\ \dfrac{|n|-1+\alpha}{\alpha}\operatorname{sign} n, & |n| > n_0. \end{cases} \tag{A5}$$

At $|k| \leqslant 1$ and $k \neq 0$, it yields

$$p = \begin{cases} n, & |n| \leqslant n_1 \\ \dfrac{a_1 - \sqrt{a_1^2 - 4a_0(a_2+|n|)}}{2a_0}\operatorname{sign} n, & n_1 < |n| \leqslant n_2 \\ \dfrac{|n|-1+\alpha}{\alpha}\operatorname{sign} n, & |n| > n_2. \end{cases} \tag{A6}$$

For $|k| > 1$, we derive

$$p = \begin{cases} \dfrac{n}{\alpha+\dfrac{1-\alpha}{|k|}}, & |n| \leqslant n_3 \\ \dfrac{a_1 - \sqrt{a_1^2 - 4a_0(a_2+|n|)}}{2a_0}\operatorname{sign} n, & n_3 < |n| \leqslant n_2 \\ \dfrac{|n|-1+\alpha}{\alpha}\operatorname{sign} n, & |n| > n_2. \end{cases} \tag{A7}$$

A.3. The constitutive moment, $M_C(x, \varepsilon(x), \varphi'(x)) = M_Y m(p, k, \alpha)$

The constitutive bending moment is defined by (7c). Here it will be given as a function of p, k, and α. Expressing m as a function of n, k, and α, as usually needed in the finite element method, is straightforward by application of (A2)–(A4). The derivation is similar as in Subsections A.1 and A.2, and will, therefore, be omitted.

For $k = 0$, we obtain

$$m = 0, \quad p \in \mathbb{R}. \tag{A8}$$

For $|k| \leqslant 1$ and $k \neq 0$, the constitutive moment is

$$m = \begin{cases} k, & |p| \leqslant p_1 \\ (1-\alpha)\dfrac{1-|p|}{4}\left(3-\dfrac{(1-|p|)^2}{k^2}\right)\operatorname{sign} k + \dfrac{1+\alpha}{2}k, & p_1 < |p| \leqslant p_2 \\ \alpha k, & |p| > p_2. \end{cases} \tag{A9}$$

Finally, for $|k| > 1$, the constitutive moment takes the form

$$m = \begin{cases} \dfrac{1-\alpha}{2}\left(3-\dfrac{1+3p^2}{k^2}\right)\operatorname{sign} k + \alpha k, & |p| \leqslant p_3 \\ (1-\alpha)\dfrac{1-|p|}{4}\left(3-\dfrac{(1-|p|)^2}{k^2}\right)\operatorname{sign} k + \dfrac{1+\alpha}{2}k, & p_3 < |p| \leqslant p_2 \\ \alpha k, & |p| > p_2. \end{cases} \tag{A10}$$

Note that expressions (A9) at $|p| \leqslant p_1$, and (A10) at $|p| \leqslant p_3$, for $p = 0$ and $\alpha = 0$ reduce to the ones usually observed in literature for constitutive bending moment M_C when axial and shear forces are neglected, refer to Liu et al. (1989) and Yu and Johnson (1982b). Expressions (A8)–(A10) hold true even for $\alpha = 0$ ($E_p = 0$); yet extensional strain ε does not exist then (see Subsection A.2). Notice, furthermore, that m is an even function of p, and an odd one of k.

A.4. The cross-sectional constitutive matrix, $\mathbf{C}(p, k, \alpha)$

The cross-sectional constitutive matrix is defined by

$$\mathbf{C} \equiv \begin{bmatrix} \dfrac{\partial N_C}{\partial \varepsilon} & \dfrac{\partial N_C}{\partial \varphi'} \\ \dfrac{\partial M_C}{\partial \varepsilon} & \dfrac{\partial M_C}{\partial \varphi'} \end{bmatrix} = \int_A \frac{\partial \sigma}{\partial D}\begin{bmatrix} 1 & z \\ z & z^2 \end{bmatrix} \mathrm{d}A. \tag{A11}$$

Thermodynamical considerations demand that the constitutive matrix must be positive definite (see, e.g., Antman and Rosenfeld, 1978). The elements of $\mathbf{C}$ are denoted by C_{11}, C_{22}, and $C_{12} = C_{21}$, and are termed tangent stiffnesses of the cross-section. The positive definiteness of $\mathbf{C}$ assures the validity of the implicit function theorem needed when employed in (8) or in (A5)–(A7). We omit the details of the derivation of (A11), because it is similar as in the previous subsections.

To derive $\mathbf{C}$ in a nondimensional form, we introduce matrix $\mathbf{B}$ with components B_{11}, $B_{12} = B_{21}$, and B_{22} by

$$\mathbf{C} = \begin{bmatrix} A_E B_{11} & S_E B_{12} \\ S_E B_{21} & I_E B_{22} \end{bmatrix},$$

where $A_E = bhE$, $S_E = bh^2E/2$, and $I_E = bh^3E/12$.

For $k = 0$, we derive

$$\mathbf{B} = \begin{cases} \begin{bmatrix} 1 & 0 \\ 0 & 1 \end{bmatrix}, & |p| \leqslant p_0 \\ \begin{bmatrix} \alpha & 0 \\ 0 & \alpha \end{bmatrix}, & |p| > p_0, \end{cases} \tag{A12}$$

for $|k| \leqslant 1$ and $k \neq 0$, (A11) gives

$$\mathbf{B} = \begin{cases} \begin{bmatrix} 1 & 0 \\ 0 & 1 \end{bmatrix}, & |p| \leqslant p_1 \\ \begin{bmatrix} (1-\alpha)\dfrac{1-|p|}{2|k|} + \dfrac{1+\alpha}{2} & \dfrac{1-\alpha}{4}\left(\dfrac{(1-|p|)^2}{k^2} - 1\right)\operatorname{sign}(kp) \\ \dfrac{1-\alpha}{4}\left(\dfrac{(1-|p|)^2}{k^2} - 1\right)\operatorname{sign}(kp) & (1-\alpha)\dfrac{(1-|p|)^3}{2|k|^3} + \dfrac{1+\alpha}{2} \end{bmatrix}, & p_1 < |p| \leqslant p_2 \\ \begin{bmatrix} \alpha & 0 \\ 0 & \alpha \end{bmatrix}, & |p| > p_2, \end{cases} \tag{A13}$$

for $|k| > 1$, the constitutive matrix is expressed by

$$\mathbf{B} = \begin{cases} \begin{bmatrix} \dfrac{1-\alpha}{|k|} + \alpha & -p\dfrac{1-\alpha}{k^2}\operatorname{sign} k \\ -p\dfrac{1-\alpha}{k^2}\operatorname{sign} k & (1-\alpha)\dfrac{1+3p^2}{|k|^3} + \alpha \end{bmatrix}, & |p| \leqslant p_3 \\ \begin{bmatrix} (1-\alpha)\dfrac{1-|p|}{2|k|} + \dfrac{1+\alpha}{2} & \dfrac{1-\alpha}{4}\left(\dfrac{(1-|p|)^2}{k^2} - 1\right)\operatorname{sign}(kp) \\ \dfrac{1-\alpha}{4}\left(\dfrac{(1-|p|)^2}{k^2} - 1\right)\operatorname{sign}(kp) & (1-\alpha)\dfrac{(1-|p|)^3}{2|k|^3} + \dfrac{1+\alpha}{2} \end{bmatrix}, & p_3 < |p| \leqslant p_2 \\ \begin{bmatrix} \alpha & 0 \\ 0 & \alpha \end{bmatrix}, & |p| > p_2. \end{cases} \tag{A14}$$

Appendix B: The Jacobian matrix, $D\mathbf{g}(\mathbf{x})$

Notations: D, the derivative operator; $\mathbf{x}$, the vector of unknown variables

$$\mathbf{x} = (y_2, \ldots, y_{n-1}, \Lambda_1^0, \Lambda_2^0, u_1, u_2, u_3 \equiv y_1, u_4, u_5, u_6 \equiv y_n)$$

of the collocation method; and $\mathbf{g}$, the vector-valued function of approximate equilibrium equations derived in Section 3. We assume that the collocation points span the interval $[-1, 1]$. The present discussion is limited to conservative distributed loads defined by functions $\mathscr{P}_x = \mathscr{P}_x(x)$, $\mathscr{P}_z = \mathscr{P}_z(x)$, and $\mathscr{M} = \mathscr{M}(x)$.

Auxiliary expressions, i.e. the derivatives of equilibrium and constitutive axial and transverse forces, and of the constitutive bending moment, are given first.

Considering expressions (12) and approximation (14), we obtain ($m = 1, \ldots, n$)

$$\begin{aligned} &\frac{\partial N}{\partial \Lambda_1^0} = \cos\tilde{\varphi}, \quad \frac{\partial N}{\partial \Lambda_2^0} = -\sin\tilde{\varphi}, \quad \frac{\partial N}{\partial y_m} = -QP_m, \\ &\frac{\partial Q}{\partial \Lambda_1^0} = \sin\tilde{\varphi}, \quad \frac{\partial Q}{\partial \Lambda_2^0} = \cos\tilde{\varphi}, \quad \frac{\partial Q}{\partial y_m} = -NP_m. \end{aligned} \tag{B1}$$

The application of (12), (14), and (8) in (5) implies

$$\begin{aligned} N(x, \Lambda_1^0, \Lambda_2^0, \tilde{\varphi}(x, \mathbf{y})) &= N_C(x, \varepsilon(x, \Lambda_1^0, \Lambda_2^0, \tilde{\varphi}(x, \mathbf{y})), \tilde{\varphi}'(x, \mathbf{y})), \\ Q(x, \Lambda_1^0, \Lambda_2^0, \tilde{\varphi}(x, \mathbf{y})) &= Q_C(x, \gamma(x, \Lambda_1^0, \Lambda_2^0, \tilde{\varphi}(x, \mathbf{y}))), \\ M_C &= M_C(x, \Lambda_1^0, \Lambda_2^0, \varepsilon(x, \Lambda_1^0, \Lambda_2^0, \tilde{\varphi}(x, \mathbf{y})), \tilde{\varphi}'(x, \mathbf{y})). \end{aligned} \tag{B2}$$

Therefore, the derivatives of ε, γ, and M_C with respect to Λ_1^0, Λ_2^0, and $\mathbf{y}$ are given through (B2), (B1), and the condition $C_{11} \neq 0$, which is obtained from the implicit function theorem, using formulae

$$\begin{aligned} &\frac{\partial \varepsilon}{\partial \Lambda_1^0} = \frac{\cos\tilde{\varphi}}{C_{11}}, \quad \frac{\partial \varepsilon}{\partial \Lambda_2^0} = -\frac{\sin\tilde{\varphi}}{C_{11}}, \quad \frac{\partial \varepsilon}{\partial y_m} = -\frac{QP_m}{C_{11}} - 2\frac{C_{12}P_m'}{LC_{11}}, \\ &\frac{\partial \gamma}{\partial \Lambda_1^0} = \frac{\sin\tilde{\varphi}}{A_G}, \quad \frac{\partial \gamma}{\partial \Lambda_2^0} = \frac{\cos\tilde{\varphi}}{A_G}, \quad \frac{\partial \gamma}{\partial y_m} = -\frac{NP_m}{A_G}, \\ &\frac{\partial M_C}{\partial \Lambda_1^0} = \frac{C_{12}}{C_{11}}\cos\tilde{\varphi}, \quad \frac{\partial M_C}{\partial \Lambda_2^0} = -\frac{C_{12}}{C_{11}}\sin\tilde{\varphi}, \quad \frac{\partial M_C}{\partial y_m} = 2\frac{\det \mathbf{C}}{LC_{11}}P_m' - \frac{C_{12}}{C_{11}}QP_m, \end{aligned}$$

where $m = 1, \ldots, n$.

The nonvanishing members of Jacobian matrix $D\mathbf{g}(\mathbf{x})$ are:

$$\frac{\partial g_1}{\partial \Lambda_1^0} = -\frac{L}{2}\int_{-1}^{1}\left(\frac{\cos^2\tilde{\varphi}}{C_{11}}+\frac{\sin^2\tilde{\varphi}}{A_G}\right)\mathrm{d}x,$$

$$\frac{\partial g_1}{\partial \Lambda_2^0} = \frac{\partial g_2}{\partial \Lambda_1^0} = \frac{L}{2}\int_{-1}^{1}\left(\frac{1}{C_{11}}-\frac{1}{A_G}\right)\sin\tilde{\varphi}\cos\tilde{\varphi}\,\mathrm{d}x,$$

$$\frac{\partial g_2}{\partial \Lambda_2^0} = -\frac{L}{2}\int_{-1}^{1}\left(\frac{\sin^2\tilde{\varphi}}{C_{11}}+\frac{\cos^2\tilde{\varphi}}{A_G}\right)\mathrm{d}x,$$

$$\frac{\partial g_1}{\partial y_m} = \int_{-1}^{1}\frac{C_{12}}{C_{11}}P_m'\cos\tilde{\varphi}\,\mathrm{d}x+\frac{L}{2}\int_{-1}^{1}\left(Q\frac{\cos\tilde{\varphi}}{C_{11}}-N\frac{\sin\tilde{\varphi}}{A_G}\right)P_m\,\mathrm{d}x$$

$$+\frac{L}{2}\int_{-1}^{1}((1+\varepsilon)\sin\tilde{\varphi}-\gamma\cos\tilde{\varphi})P_m\,\mathrm{d}x,$$

$$\frac{\partial g_2}{\partial y_m} = -\int_{-1}^{1}\frac{C_{12}}{C_{11}}P_m'\sin\tilde{\varphi}\,\mathrm{d}x-\frac{L}{2}\int_{-1}^{1}\left(Q\frac{\sin\tilde{\varphi}}{C_{11}}+N\frac{\cos\tilde{\varphi}}{A_G}\right)P_m\,\mathrm{d}x$$

$$+\frac{L}{2}\int_{-1}^{1}((1+\varepsilon)\cos\tilde{\varphi}+\gamma\sin\tilde{\varphi})P_m\,\mathrm{d}x,$$

$$\frac{\partial g_{k+2}}{\partial \Lambda_1^0} = \frac{\partial M_C}{\partial \Lambda_1^0}(x_k)-\frac{\partial M_C}{\partial \Lambda_1^0}(x_{k-1})-\frac{L}{2}\int_{x_{k-1}}^{x_k}\left(Q\frac{\cos\tilde{\varphi}}{C_{11}}-N\frac{\sin\tilde{\varphi}}{A_G}\right)\mathrm{d}x$$

$$-\frac{L}{2}\int_{x_{k-1}}^{x_k}((1+\varepsilon)\sin\tilde{\varphi}-\gamma\cos\tilde{\varphi})\,\mathrm{d}x,$$

where

$$\frac{\partial M_C}{\partial \Lambda_1^0}(x_0) = \frac{\partial M_C}{\partial \Lambda_1^0}(x_n) = 0,$$

$$\frac{\partial g_{k+2}}{\partial \Lambda_2^0} = \frac{\partial M_C}{\partial \Lambda_2^0}(x_k)-\frac{\partial M_C}{\partial \Lambda_2^0}(x_{k-1})+\frac{L}{2}\int_{x_{k-1}}^{x_k}\left(Q\frac{\sin\tilde{\varphi}}{C_{11}}+N\frac{\cos\tilde{\varphi}}{A_G}\right)\mathrm{d}x$$

$$-\frac{L}{2}\int_{x_{k-1}}^{x_k}((1+\varepsilon)\cos\tilde{\varphi}+\gamma\sin\tilde{\varphi})\,\mathrm{d}x,$$

where

$$\frac{\partial M_C}{\partial \Lambda_2^0}(x_0) = \frac{\partial M_C}{\partial \Lambda_2^0}(x_n) = 0,$$

$$\frac{\partial g_{k+2}}{\partial \Lambda y_m} = \frac{\partial M_C}{\partial y_m}(x_k) - \frac{\partial M_C}{\partial y_m}(x_{k-1}) + \int_{x_{k-1}}^{x_k} \frac{C_{12}}{C_{11}} Q P'_m \, dx$$

$$+ \frac{L}{2} \int_{x_{k-1}}^{x_k} \left(\frac{Q^2}{C_{11}} + \frac{N^2}{A_G} \right) P_m \, dx - \frac{L}{2} \int_{x_{k-1}}^{x_k} ((1+\varepsilon)N + \gamma Q) P_m \, dx,$$

where

$$\frac{\partial M_C}{\partial y_m}(x_0) = \frac{\partial M_C}{\partial y_m}(x_n) = 0$$

$$-\frac{\partial g_1}{\partial u_1} = -\frac{\partial g_2}{\partial u_2} = \frac{\partial g_1}{\partial u_4} = \frac{\partial g_2}{\partial u_5} = \frac{\partial g_{n+3}}{\partial \Lambda_1^0} = \frac{\partial g_{n+4}}{\partial \Lambda_2^0} = \frac{\partial g_{n+5}}{\partial \Lambda_1^0} = \frac{\partial g_{n+6}}{\partial \Lambda_2^0} = 1,$$

where $m, k = 1, \ldots, n$. All derivatives of M_C at x_0 and x_n vanish in accord with the natural boundary conditions (4c) and (4f). The Jacobian matrix is not symmetric, and the stability of its inversion is influenced by the choice of the set of collocation points $\{x_k\}_{k \in I_{n+1}}$.

References

Antman, S. S. and Rosenfeld, G. (1978) Global behavior of buckled states of non-linearly elastic rods. *SIAM Review* **20,** 513–566 and **22,** 186–187 (1980).

Bayliss, A. and Matkowsky, B. J. (1987) Fronts, relaxation oscillations, and period doubling in solid fuel combustion. *J. Comput. Phys.* **71,** 147–168.

Bayliss, A., Gottlieb, D., Matkowsky, B. J. and Minkoff, M. (1989) An adaptive pseudo-spectral method for reaction diffusion problems. *J. Comput. Phys.* **81,** 421–443.

Coulter, B. A. and Miller, R. E. (1989) Loading, unloading and reloading of a generalized plane plastica. *International Journal of Numerical Methods in Engineering* **28,** 1645–1660.

Cowper, G. R. (1966) The shear coefficient in Timoshenko's beam theory. *ASME Journal of Applied Mechanics* **33,** 335–340.

Fried, I. (1985) Large-deflection computation of the plastica. *Comput. Methods Appl. Mech. Engrg* **49,** 163–173.

Guillard, H. and Peyret, R. (1988) On the use of spectral methods for the numerical solution of stiff problems. *Comput. Methods Appl. Mech. Engrg* **66,** 17–43.

Hutchinson, J. W. and Koiter, W. T. (1970) Postbuckling theory. *Applied Mechanics Review* **23,** 1353–1366.

Liu, J. H., Stronge, W. J. and Yu, T. X. (1989) Large deflections of an elastoplastic strain-hardening cantilever. *ASME Journal of Applied Mechanics* **56,** 737–743.

Lucas, T. R. and Reddien Jr, G. W. (1972) Some collocation methods for nonlinear boundary value problems. *SIAM J. Numer. Anal.* **9,** 341–356.

Monasa, F. (1980) Deflections of postbuckled unloaded elasto-plastic thin vertical columns. *International Journal of Solids and Structures* **16,** 757–765.

Reid, S. R. and Reddy, T. Y. (1978) Effect of strain hardening on the large plastic deformation of a cantilever. *ASME Journal of Applied Mechanics* **45,** 953–955.

Reissner, E. (1972) On one-dimensional finite-strain beam theory: the plane problem. *Z. angew. Math. Phys.* **23,** 795–804.

Russell, R. D. and Shampine, L. F. (1972) A collocation method for boundary value problems. *Numer. Math.* **19,** 1–28.

Saje, M. (1990) A variational principle for finite planar deformation of straight slender elastic beams. *International Journal of Solids and Structures* **26,** 887–900.

Saje, M. (1991) Finite element formulation of finite planar deformation of curved elastic beams. *Comput. Struct.* **39,** 327–337.

Saje, M. and Srpčič, S. (1985) Large deformations of in-plane beam. *International Journal of Solids and Structures* **21,** 1181–1195.

Saje, M., Turk, G., Kalagasidu, A. and Vratanar, B. (1998) A kinematically exact finite element formulation of elastic–plastic curved beams. *Comput. Struct.* (in press)

Saje, M., Planinc, I., Turk, G. and Vratanar, B. (1997) A kinematically exact finite element formulation of planar elastic–plastic frames. *Comput. Methods Appl. Mech. Engrg* **144,** 125–151.

Tvergaard, V. and Needleman, A. (1980) On the localization of buckling patterns. *ASME Journal of Applied Mechanics* **47,** 613–619.

Wu, X. Q. and Yu, T. X. (1986) The complete process of large elastic–plastic deflection of a cantilever. *Acta Mech. Sinica* **2,** 333–347.

Yu, T. X. and Johnson, W. (1982a) The plastica: the large elastic–plastic deflection of a strut. *Int. J. Non-Linear Mech.* **17,** 195–209.

Yu, T. X. and Johnson, W. (1982b) Influence of axial force on the elastic–plastic bending and springback of a beam. *J. Mech. Work. Tech.* **6,** 5–21.

Zemanian, A. H. (1987) *Distribution Theory and Transform Analysis.* Dover Publications, Inc., New York.